Available online at www.sciencedirect.com
SCIENCE DIRECT®
ELSEVIER
Earth and Planetary Science Letters 218 (2004) 347–361
EPSL
www.elsevier.com/locate/epsl

Sulfur chemistry in laser-simulated impact vapor clouds: implications for the K/T impact event

Sohsuke Ohno [a,*], Seiji Sugita [a], Toshihiko Kadono [b], Sunao Hasegawa [c], George Igarashi [d,1]

[a] *Department of Earth and Planetary Science, Graduate School of Science, University of Tokyo, 7-3-1 Hongo Bunkyo-ku, Tokyo 113-0033, Japan*

[b] *Institute for Frontier Research on Earth Evolution, Japan Marine Science and Technology, 2-15 Natsushima, Yokosuka, Kanagawa 237-0061, Japan*

[c] *Department of Planetary Science, Institute of Space and Astronautical Science, Japan Aerospace Exploration Agency, 3-1-1 Yoshinodai, Sagamihara, Kanagawa 229-8510, Japan*

[d] *Laboratory for Earthquake Chemistry, Graduate School of Science, University of Tokyo, 7-3-1 Hongo Bunkyo-ku, Tokyo 113-0033, Japan*

Received 20 September 2002; received in revised form 22 September 2003; accepted 26 November 2003

Abstract

One of the most promising mechanisms for the mass extinction at the K/T boundary event is blockage of sunlight by sulfuric acid aerosol, which is induced by impact vaporization of sulfate in evaporite deposits around the K/T impact site. One of the advantages of this hypotheses is that it may cause an impact winter much longer than that by silicate dust and soot due to a global wildfire. However, the residence time of sulfuric acid aerosol in the stratosphere depends strongly on the ratio of SO_2/SO_3 in the K/T impact vapor. If SO_3 was dominant, the blockage of sunlight by the sulfuric acid aerosol would not last longer than that by silicate dust and soot. The chemical reaction of sulfur oxides in an impact vapor cloud has not been studied extensively before. This study carries out chemical equilibrium calculations, kinetic model calculations, and laser irradiation experiments with a quadrupole mass spectrometer to estimate the SO_2/SO_3 ratio in the K/T impact vapor cloud. The results strongly suggest that most of sulfur oxides in the K/T impact vapor cloud may have been SO_3, not SO_2. The sulfuric acid aerosol may not have been able to block the sunlight for a long time.

Keywords: K/T boundary; impact vapor cloud; sulfuric acid aerosol; mass spectroscopy; chemical reaction

1. The role of the SO_2/SO_3 ratio in the K/T event

A large bolide impact is widely accepted as the cause of the K/T mass extinction event. After the discovery of the global distribution of Ir anomaly by Alvarez et al. [1], several additional supporting lines of evidence have been found. These include the global distribution of coeval shocked quartz

* Corresponding author. Tel.: +81-3-5841-4300; Fax: +81-3-5841-8075.
E-mail address: oono@eps.s.u-tokyo.ac.jp (S. Ohno).

[1] Present address: Research Center for Prediction of Earthquakes and Volcanic Eruptions, Graduate School of Science, Tohoku University, Aoba-ku, Sendai, 980-8578, Japan.

0012-821X/03/$ – see front matter © 2003 Elsevier B.V. All rights reserved.
doi:10.1016/S0012-821X(03)00687-3

(e.g., [2]) and the Chicxulub crater (e.g., [3]). Furthermore, both the crystallization ages and stable isotopic compositions are consistent between the impact melt inside the Chicxulub crater and the impact glass [4] in the K/T boundary layer around the globe.

However, there is still significant controversy over the exact extinction mechanism resulting from this impact. An initial hypothesis proposed that silicate dust was injected by the impact into stratosphere and blocked the sunlight [1,5,6]. However, silicate dust could not stay in the atmosphere for a long time, possibly only several months (e.g., [7]). This duration of sunlight blockage may have been too short to cause a K/T-size mass extinction.

More recently, a large amount of impact glasses rich in both Ca and SO_3 were found in Haiti [8], which indicates that a large amount of sulfur may have been degassed during the K/T impact event from the sulfate-rich Yucatan sediments. The degassed sulfur converts to sulfuric acid aerosol and stays in the stratosphere for a long time. Because of the large quantity of degassed sulfur in the K/T impact event, this would have reduced the sunlight significantly [9–14]. This effect may have lasted for several years and led to a mass extinction. Because of its longer duration of insolation blockage than that of silicate dust scenario or soot scenario (e.g., [15]), the sulfuric acid aerosol is considered to be one of the most cogent mechanisms for the K/T mass extinction.

However, the residence time of sulfuric acid aerosol in the stratosphere changes dramatically depending on whether the impact-released sulfur oxides is dominated by SO_2 or SO_3 (e.g., [10]). In the stratosphere, SO_2 converts to sulfuric acid aerosol via SO_3. The conversion time scale of SO_2 to SO_3 is much longer than that of SO_3 to sulfuric acid aerosol (e.g., [16]). If most of degassed sulfur was SO_2, blockage of the sunlight by sulfuric acid aerosol would have lasted for several years. However, if most of degassed sulfur was SO_3, sulfuric acid aerosol could not block the sunlight for such a long time. SO_3 would react with water, which was rich in the K/T impact vapor cloud, and be converted to sulfuric acid aerosol immediately (e.g., [10]). Once the degassed sulfur is converted to sulfuric acid aerosol, aerosol particles fall from the stratosphere as quickly as silicate dust. Then, sulfuric acid aerosol cannot block the sunlight for a long time and may not be able to cause a K/T-scale mass extinction.

Thus the SO_2/SO_3 ratio of the impact vapor cloud is critical in assessing the sulfuric acid model. The key process to determine the final SO_2/SO_3 ratio is quenching. An impact vapor cloud is generally in a local chemical equilibrium during early stages of its expansion because it has extremely high temperature and pressure. The high temperature and pressure maintain the rate of chemical reaction so high that change in equilibrium composition due to adiabatic expansion of impact vapor cloud can be adjusted instantaneously; chemical equilibrium hold. However, as the vapor cloud expands and decreases in temperature and pressure, it begins to take longer time to attain chemical equilibrium. After temperature and pressure of the vapor cloud becomes low enough, the chemical reaction ceases to catch up with expansion, and quenching occurs. After quenching, chemical composition does not change. Thus, an accurate estimate of both temperature and pressure at which reactions of sulfur oxides quench is the key in estimating the terminal SO_2/SO_3 ratio in an impact vapor cloud. Establishing the kinetics of sulfur oxides in vapor plumes is essential in estimating the quenching temperature of reactions of sulfur oxides in vapor clouds. However, the chemical reaction of sulfur oxides in a hot impact vapor plume has not been studied extensively before. The experimental study by Tyburczy and Ahrens [17] suggests that impact vaporization of anhydrite may release mainly SO_2 gas. However, deposition plate analyses after laser irradiation experiments by Gerasimov et al. [18] and Ivanov et al. [9] suggest that degassed gas will be dominated by SO_3. Since there has been no direct analysis of gas-phase products, it is still uncertain whether the degassing product of evaporite is dominated by SO_2 or SO_3.

The goal of this study is to understand the kinetics of sulfur oxides in impact-induced vapor clouds. To achieve this goal we took three approaches, chemical equilibrium calculations, kinetic calculations, and laser ablation experiments.

Here it should be noted that experiments in this study are not intended to simulate directly the chemical reactions in the K/T impact vapor cloud but to obtain basic data on the chemical reaction process among sulfur oxides in a high temperature vapor cloud. In the following, we first discuss the calculation of the equilibrium composition of sulfur oxides along different adiabatic decompression curves (p–T curves) following impacts. Second, the kinetics of the chemical reaction is assessed with a theoretical model based on kinetic parameters in the literature. Third, we carry out mass spectroscopic analysis of vapor plumes created by laser irradiation on anhydrite ($CaSO_4$). Fourth, we discuss the geologic implications for the K/T impact event based on a preliminary kinetic model inferred from the experimental results.

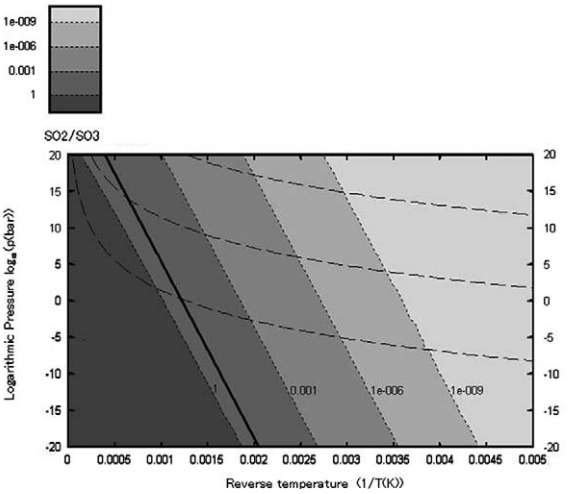

Fig. 1. The results of the chemical equilibrium calculations. Contours show the SO_2/SO_3 ratio obtained with Gibbs free energy minimization. The thick black line shows the p–T conditions for a constant SO_2/SO_3 ratio, derived from a simplified analytical approach using the Clausius–Clapeyron relation (see Appendix). The dashed curves show adiabatic decompression paths of ideal gases with different initial conditions (see Appendix). Note that the contours are parallel to the black line and that every ideal-gas decompression path (i.e., dashed curve) extends to the far right (i.e., a very low SO_2/SO_3 ratio). The equilibrium SO_2/SO_3 ratio decreases as a vapor cloud expands regardless of its initial peak-shock condition.

2. Chemical equilibrium calculations

We carried out chemical equilibrium calculations to determine the SO_2/SO_3 ratio in vapor clouds, using the Gibbs free energy minimization method [19] and JANAF thermochemical tables [20]. The assumptions in our chemical equilibrium calculations are the following. (1) The impact vapor in the calculations is assumed to be always in a chemical equilibrium. (2) The initial temperature of vapor clouds is higher than 3000 K. CaO in the system has already condensed when the temperature of the vapor clouds decreases below 3000 K. (3) The molar ratio of Ca to S to O is assumed to be 1:1:4 in the initial vapor cloud (i.e., $CaSO_4$). Since CaO condenses at high temperatures, the entire initial Ca and a quarter of the initial O are removed from the gas phase of the vapor cloud at temperatures lower than 3000 K. Thus the molar ratio of S to O in the gas phase at the temperatures we consider here is fixed at 1:3. (4) SO_2, SO_3, SO, S, O, and O_2 are assumed to be the dominant species in the vapor cloud; other species are negligible. The results of the calculations are shown in Fig. 1.

To estimate the SO_2/SO_3 ratio in the K/T impact vapor cloud, we assumed several different impact velocities and different types of projectiles for the K/T impact. The initial temperature and pressure of a vapor cloud are determined with the Rankine–Hugoniot relation and the linear shock–particle velocity relation [21]. Decreasing temperature and pressure of the vapor cloud in subsequent adiabatic expansion phase are calculated with an ideal-gas equation of state. Both molecular weight μ and the ratio γ of heat capacities are determined by the chemical equilibrium calculations at each temperature and pressure condition. The assumption of ideal gas is not accurate at high pressures. Thus the temperature–pressure relation obtained in these calculations may have a significant error near the initial conditions of impact vapor clouds. Nevertheless, the ideal equation of state holds well under temperature and pressure conditions where the chemical reactions among sulfur oxides may freeze.

The results of the calculations indicate that SO_2+O is more stable at high temperatures and

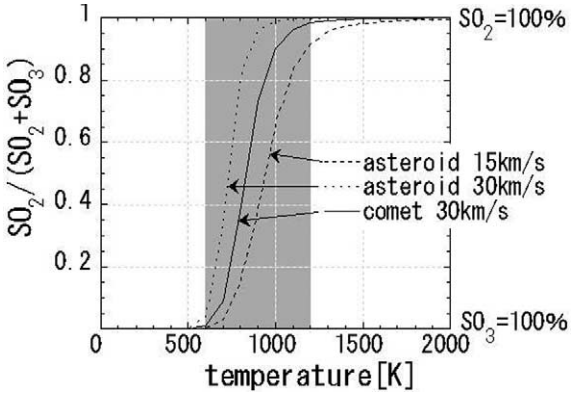

Fig. 2. The chemical equilibrium of sulfur oxides for possible impact conditions for the K/T impact vapor cloud. The $SO_2/(SO_2+SO_3)$ ratio is shown as a function of temperature. The hatched area in the figure corresponds to the temperature range where the sulfur oxidation state changed dramatically.

high pressures and that SO_3 is more stable at low temperatures and low pressures (Fig. 2). This general trend holds over a very wide range of initial conditions of vapor (see Appendix). Over the entire range of the impact conditions we assumed the SO_2/SO_3 ratio dramatically changes in the range between 600 and 1200 K. If the reaction SO_2+O to SO_3 quenches at a temperature higher than 1200 K, most of impact-degassed sulfur is released to the environment as SO_2. Then, its conversion to sulfuric acid aerosol will take place slowly. However, if the reaction SO_2+O to SO_3 quenches at a temperature lower than 600 K, SO_3 is dominant.

3. Kinetic estimation of the SO_2/SO_3 ratio

The results of the chemical equilibrium calculations above established the relation between the quenching temperature and the terminal SO_2/SO_3 ratio in an impact vapor cloud. However, sulfur oxides kinetics is necessary for estimation of the quenching temperature. We carried out model calculations of the sulfur oxides kinetics in expanding vapor clouds.

3.1. Quenching temperature

Competition between the rate of chemical reaction and the rate of change in equilibrium composition due to adiabatic expansion determines whether equilibrium holds or not:

$$\left(\frac{\mathrm{d}[\mathrm{SO_3}]}{\mathrm{d}t}\right)_{\mathrm{re}} \geq \left(\frac{\mathrm{d}[\mathrm{SO_3}]}{\mathrm{d}t}\right)_{\mathrm{eq}} \tag{1}$$

where $(\mathrm{d}[SO_3]/\mathrm{d}t)_{eq}$ is the rate of change in the equilibrium abundance of SO_3 in an adiabatically expanding vapor cloud, and $(\mathrm{d}[SO_3]/\mathrm{d}t)_{re}$ is the chemical reaction rate controlled by the kinetics. Immediately after impact, equilibration occurs quickly and the inequality holds. Then, as the vapor expands, at a certain point the equality is met and the vapor is quenched (i.e., chemical reactions are assumed to stop). The equality in Eq. 1 holds at the quenching temperature. Since the equilibrium chemical composition is not a direct function of time but of thermodynamic variables such as volume V and entropy S, we rewrite the right-hand side of Eq. 1 using three variables. Then the equality of Eq. 1 becomes:

$$\frac{\left(\frac{\mathrm{d}[\mathrm{SO_3}]}{\mathrm{d}t}\right)_{\mathrm{re}}}{\left(\frac{\mathrm{d}V}{\mathrm{d}t}\right)_{\mathrm{s}}} = \left(\frac{\mathrm{d}[\mathrm{SO_3}]}{\mathrm{d}V}\right)_{\mathrm{eq}} \tag{2}$$

where $(\mathrm{d}V/\mathrm{d}t)_s$ is the adiabatic expansion rate of a vapor cloud and $(\mathrm{d}[SO_3]/\mathrm{d}V)_{eq}$ is the volume derivative of the equilibrium abundance of SO_3. The solution of Eq. 2 gives the quenching temperature for a given condition of vapor cloud.

The rate of reaction and the change in equilibrium chemical composition are calculated along adiabatic p–T curves. Pressure along an adiabatic p–T curve at each temperature is calculated based on the conservation of entropy, where the entropy is determined with the chemical equilibrium calculations. The entropy of a mixture of ideal gas is given by Prigogine and Defay [19].

3.2. Vapor expansion

A vapor cloud is assumed to have a hemispherical shape and to expand at the sound velocity, which changes as a function of time. The rate of change in the volume of a vapor cloud is given by:

$$\left(\frac{dV}{dt}\right)_s = 2\pi r^2 C_s \quad (3)$$

or

$$\left(\frac{dV}{dt}\right)_s = (18\pi)^{\frac{1}{3}} V^{\frac{2}{3}} C_s \quad (4)$$

where C_s, r and V are the sound velocity of the vapor cloud, the radius of the vapor cloud and the volume of the vapor cloud. The K/T impact vapor cloud is expected to have grown larger than 1000 km in diameter at the quenching temperature. It was too large to receive the effect of atmospheric pressure.

When the volume of an expanding vapor cloud is determined, its temperature T and pressure can be calculated with an ideal-gas equation of state under an adiabatic condition:

$$\frac{T}{T_0} = \left(\frac{V}{V_0}\right)^{1-\gamma} \quad (5)$$

where T_0 and V_0 are the temperature and volume of the vapor cloud before expansion (i.e., immediately after the impact). The ratio γ of specific heats is calculated based on the chemical composition of the vapor as a function of time. It is also noted that dimensional analysis of Eq. 1 shows that a characteristic timescale for the expansion of the vapor cloud is proportional to the initial radius r_0 of impact vapor cloud. Thus the rate of change in temperature and pressure is proportional to $1/r_0$ and $M_0^{-1/3}$, where M_0 is the vapor mass.

3.3. Chemical reaction rate

Although there may be a number of chemical reactions to convert SO_2 to SO_3, we consider only the reaction:

$$SO_2 + O + M \rightarrow SO_3 + M \quad (6)$$

in this study. Other reaction paths are not considered in this study, because there are no data on the reaction rate coefficient at high temperatures. The formation rate of $[SO_3]$ is determined by a formula by Troe [22]:

$$\frac{d[SO_3]}{dt} = k[SO_2][O][M] \quad (7)$$

where k is the rate coefficient of Eq. 6. If the third body M in Eq. 6 is argon, k is given by:

$$k/[\mathrm{Ar}] \cong 10^{16.6}\left(\frac{T}{1000\ \mathrm{K}}\right)^{-4} \exp$$

$$(-22\ \mathrm{kJ\ mol^{-1}}/RT) \times (\mathrm{cm^6\ mol^{-1}\ s^{-1}}) \quad (8)$$

Here we consider as SO_2, which is the most abundant molecular species in the model in this study. The ratio of $k(M = Ar)/k(M = SO_2)$ is 0.71/6.9 [23]. The abundances of SO_2 and O are assumed to be determined by the chemical equilibrium composition.

The model in this study gives a lower limit for the reaction rate. In other words, the estimated SO_2/SO_3 ratio in this model gives an upper limit of the SO_2/SO_3 ratio in an impact vapor cloud. First, if reaction paths other than the one considered here exist, the total rate of the reaction from SO_2 to SO_3 is underestimated in the model. Second, the actual abundance of O is higher than the abundance given by the equilibrium chemical composition, which is used in the model calculations. The equilibrium abundance of O decreases as the temperature decreases. If the reaction SO_2 to SO_3 is very slow and the abundance of O freezes at higher temperatures than the quenching temperature of Eq. 6, the abundance of O is higher than that of the equilibrium chemical composition at the quenching temperature of Eq. 6. In contrast, if the reaction SO_2 to SO_3 is very fast, the SO_2/SO_3 ratio in a vapor cloud converges quickly to the equilibrium chemical ratio. The abundance of O in a vapor cloud cannot be smaller than that of the equilibrium chemical composition at a given temperature.

3.4. Calculation results

Fig. 3 shows the results of the kinetic model calculations. We estimated the SO_2/SO_3 ratio at the quenching temperatures as a function of the mass of a vapor. Because a larger vapor cloud cools down more slowly, its quenching temperature is lower. Therefore, the terminal SO_2/SO_3 ratio is smaller for a vapor cloud with a larger mass.

The SO_2/SO_3 ratio in a K/T-size vapor cloud is

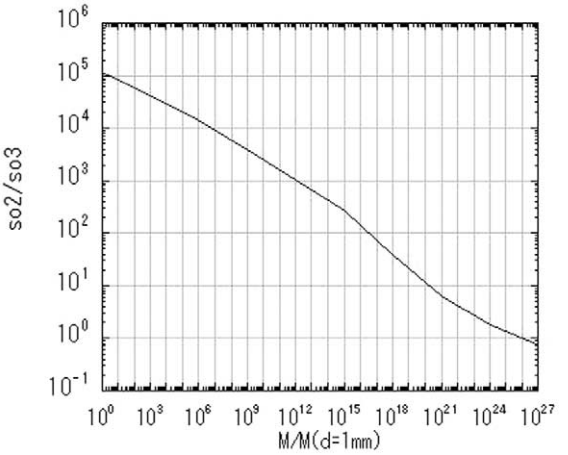

Fig. 3. The results of the theoretical model calculations of the kinetics of sulfur oxides. The SO_2/SO_3 ratio at the quenching temperature is shown as a function of the mass of the vapor cloud. The mass of a vapor cloud is normalized by the mass of the vapor cloud generated by laser irradiation at 1 mm beam diameter. The SO_2/SO_3 ratio in K/T-size vapor cloud (i.e., 10^{25}–10^{26} times larger than that in the laser irradiation experiment) is approximately 1. The mass of the K/T impact vapor cloud is based on Pope et al. [11].

approximately unity. This result is significantly different from the standard sulfuric acid aerosol scenario of K/T mass extinction (e.g., [11]), in which most of sulfur in the vapor cloud is assumed to exist as SO_2 at the end of the vapor expansion. However, if the SO_2/SO_3 ratio was unity, the mass of SO_2 in the K/T impact vapor cloud was not largely different from previous scenarios (e.g., [10,11]). Nevertheless, the results of this kinetic model estimation give us an upper limit for SO_2/SO_3; it may be much smaller than unity.

4. Laser experiments

Because of the lack of the sufficient data on kinetics of sulfur oxide reaction, the results of the kinetic calculations in Section 3 are somewhat inconclusive. Therefore, we carried out laser irradiation experiments.

Fig. 4 shows the experimental system that we constructed for this study. A YAG laser beam was irradiated to a sample of anhydrite ($CaSO_4$) in a vacuum chamber. Vapor created by the laser irradiation is taken into a quadrupole mass spectrometer (QMS) for mass analysis. Pressure in the QMS was always kept lower than 10^{-3} Pa with a vacuum pump to ensure the linearity of the QMS analysis. We continued each experimental run until the output current of QMS became stable in order to avoid the influence of SO_2 and/or SO_3 absorbed on the walls of the vacuum chamber, QMS, and tubes.

4.1. Calibration of QMS sensitivity

The sensitivity of a QMS depends on gas species, because the ionization efficiency and the cracking pattern of each molecular species are different. Ionization of SO_2 molecules by electrons emitted from the hot filament in the QMS generates not only SO_2^+ ions (mass number 64) but also SO^+ ions (mass number 48) as well as other species of ions (e.g., S^+ and O^+), and cracking occurs. Similarly, ionization of SO_3 molecules generates not only SO_3^+ ions (mass number 80) but also SO_2^+ ions, SO^+ ions, and other species of ions. We need to know the cracking pattern in order to estimate the amount of neutral gas from a measured ion current value.

We experimentally determined the sensitivity

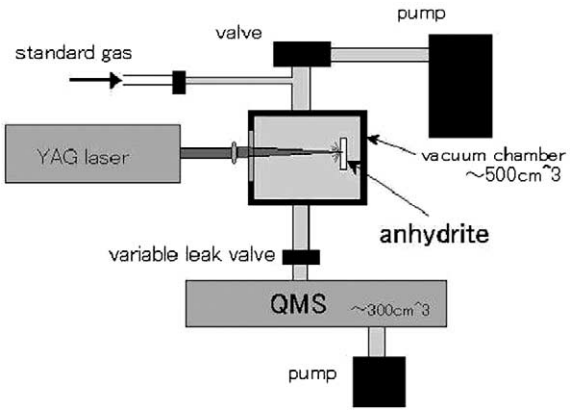

Fig. 4. Schematic diagram of the experimental system used in this study. A YAG laser beam is focused on a sample of anhydrite in the vacuum chamber. Vapor produced by laser irradiation is analyzed with a QMS. When the QMS is calibrated for its sensitivity, standard gases are introduced into the QMS.

and the cracking pattern of QMS for SO_2 and SO_3 with standard gas samples. For SO_2, a standard gas (SO_2 993 ppm, N_2 balance) was introduced to the experimental system directly from a gas cylinder. However, we could not find a commercially available gas cylinder that contains a standard SO_3 gas sample. We made a SO_3 standard gas sample by vaporizing solid state SO_3 in a vacuum chamber. The SO_3 vaporization was carried out at the room temperature. Vapor pressure of SO_3 at 298 K is 344 Torr [24]. When the standard gas sample is introduced into the QMS to calibrate its sensitivity, the pressure in the chamber is about 10^5 Pa. The variable leak valve between the vacuum chamber and the QMS was kept almost closed in order to maintain the pressure in the QMS low ($<10^{-3}$ Pa).

For the standard SO_2 sample gas, the signal for the mass–charge ratio (m/q) of 64 (i.e., SO_2^+) is 1.8 times that of 48 (i.e., SO^+). The detected SO^+ is presumably made by fragmentation of SO_2. For the standard SO_3 vaporized sample, the 64:48 ratio is comparable (1.5:1), while the current at m/q 80 is an order of magnitude lower that these.

Based on these data, we calculated the sensitivity of QMS of SO_2 and SO_3. The sensitivities of the output current values of mass numbers 64 and 48 for SO_2 are $1.20\pm0.08\times10^{-5}$ A/Pa and $6.77\pm0.65\times10^{-6}$ A/Pa, respectively. The sensitivities of the output current values of mass numbers 64, 48, and 80 for SO_3 are $4.72\pm0.20\times10^{-6}$ A/Pa, $3.17\pm0.06\times10^{-6}$ A/Pa, and $3.33\pm0.20\times10^{-7}$ A/Pa, respectively. The above errors are the standard deviations (1σ) of experimental data. All the standard deviations are smaller than a tenth of the values of sensitivity.

4.2. Laser irradiation experiments

We generated hot vapor clouds by irradiating laser beam to anhydrite targets. We analyzed the final SO_2/SO_3 ratios in vapor clouds with the QMS. The final SO_2/SO_3 ratio reflects the composition at the quenching temperature for the conversion from SO_2 to SO_3. We can obtain information on the kinetics of sulfur oxides in vapor clouds from the determined quenching temperature.

The conditions of the experiments are as follows. The pulse width and wavelength are 13 ns and 1.064 μm, respectively. The laser beam intensity on the surface of the target is 4×10^8 W/cm^2. Note that the laser intensity is not the total energy flux but the energy flux per unit area. This is approximately 1/33 of the intensity of the laser experiments by Kadono et al. [25] and near the lowest limit of the intensity to vaporize anhydrite. As we shall discuss below, the low laser intensity reproduces more realistic vapor conditions than that used by Kadono et al. [25]. Low-intensity laser irradiation also allows us to investigate a wider range of laser beam diameter for a given maximum laser output. The laser beam diameter on the surface of the target ranges from 0.4 to 1.6 mm. The lower limit of the beam diameter is constrained by the limit of the focusing optics we used. The upper limit of the beam diameter is constrained by the maximum laser pulse energy of the YAG laser. The pulse energy of the YAG laser is from 25 to 400 mJ. The repetition rate ranges from 0.3 to 3 Hz. The pressure in the main vacuum chamber was kept lower than 10^{-1} Pa in all the laser irradiation experiments.

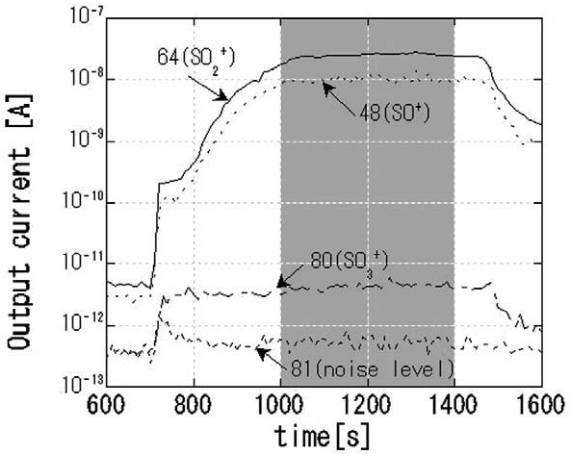

Fig. 5. The output currents of mass numbers 48, 64, 80, and 81 of a typical laser irradiation experiment. The laser beam diameter is 0.4 mm, and the pulse energy is 25 mJ. Background signals were monitored for 700 s before laser irradiation began. Although the output current of mass number 80 is nearly 6000 times smaller than that of mass number 64, the output current of mass number 80 is significantly larger than the noise level (i.e., mass number 81).

Low pressure in the chamber is necessary to simulate the adiabatic expansion of a vapor cloud into vacuum space. Low pressure also reduces the influence of reactions that the laser light absorbed by the ambient atmosphere along the laser beam path in the chamber may cause. The pressure in the QMS is kept lower than 10^{-3} Pa.

Fig. 5 shows the time series of output currents of the QMS for the mass numbers 48, 64, 80, and 81 in a laser irradiation experiment. We estimated the SO_2/SO_3 ratio in a vapor cloud from these data and the sensitivity data of the QMS discussed above. The ratio of the output current of mass number 64 to that of mass number 48 is 1.8/1. This coincides with the ratio for the SO_2 standard gas within a measurement error. Furthermore, the output current of mass number 80 is about 1/6000 of that of mass number 64. These indicate that a dominant portion of degassed sulfur is SO_2. However, the output current of mass number 80 is significantly larger than the noise level (i.e., mass number 81). Thus a significant amount of SO_3 is also produced in vapor plumes by laser irradiation. It is noted that we could not detect Ca ($m/q = 40$) or CaO ($m/q = 56$) with the QMS. Presumably CaO had condensed nearly completely in the chamber.

Fig. 6 shows the average of the output currents of mass numbers 48, 64 and 80 along with those of 49, 50, 65, 66, 81 and 82. Mass number 65 corresponds to the sum of $^{33}SO_2$ and $S^{17}OO$, mass number 66 corresponds to the sum of $^{34}SO_2$, $^{33}S^{17}OO$, $S^{17}O_2$ and $S^{18}OO$, mass number 49 corresponds to the sum of ^{33}SO and $S^{17}O$, mass number 50 corresponds to the sum of ^{34}SO, $^{33}S^{17}O$ and $S^{18}O$, mass number 81 corresponds to the sum of $^{33}SO_3$ and $S^{17}OO_2$, and mass number 82 corresponds to the sum of $^{34}SO_3$, $^{33}S^{17}OO_2$, $S^{17}O_2O$ and $S^{18}OO_2$, respectively. The ratios of the output currents of mass numbers 64 to 65, 64 to 66, 48 to 49, and 48 to 50 correspond to the isotopic abundance of sulfur (mass numbers 32, 33 and 34) and oxygen (mass numbers 16, 17 and 18) [26] (see Table 1). This coincidence unambiguously indicates that the output currents of these mass numbers correspond to SO_2 and SO in our experiment. The ratio of output currents of mass number 80 to difference between mass number 82 and noise level (i.e., mass number 81) corresponds to the isotopic ratio of sulfur and oxygen. This also supports that the output currents of mass numbers 80 and 82 reflect the abundance of SO_3 in our experiment.

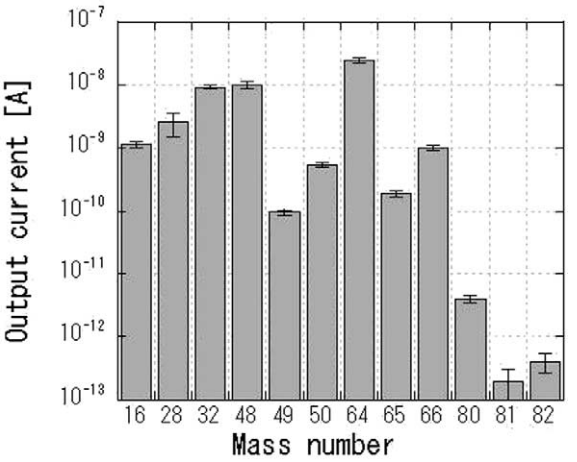

Fig. 6. The averaged output currents of mass number 16, 28, 32, 48, 49, 50, 64, 65, 66, 80, 81, and 82 of a laser irradiation experiment. The experimental condition is the same as in Fig. 4. Output currents are averaged over the period from 1000 to 1400 s, when the QMS outputs are stable. The error bars in the figure are given by the standard deviation of the time series of the output currents.

We carried out laser irradiation experiments for

Table 1
Comparison between the ratios of measured QMS output currents and those predicted from isotopic ratios of sulfur and oxygen

	Mass numbers				
	64/65	64/66	48/49	48/50	80/(82–81)
Measured	107 ± 11	21.2 ± 2.4	113 ± 18	19.9 ± 2.6	18.8 ± 15.6
Predicted[a]	114	20.3	119	21.2	19.4

[a] Species assumed from the prediction are: $^{32}S^{16}O_2$ for 64, $^{33}S^{16}O_2$ and $^{32}S^{17}O^{16}O$ for 65, $^{34}S^{16}O_2$, $^{33}S^{17}O^{16}O$, $^{32}S^{17}O_2$ and $^{32}S^{18}O^{16}O$ for 66, $^{32}S^{16}O$ for 48, $^{33}S^{16}O$ and $^{32}S^{17}O$ for 49, $^{34}S^{16}O$, $^{33}S^{17}O$, and $^{32}S^{18}O$ for 50, $^{32}S^{16}O_3$ for 80, $^{33}S^{16}O_3$ and $^{32}S^{17}O^{16}O_2$ for 81, $^{34}S^{16}O_3$, $^{33}S^{17}O^{16}O_2$, $^{32}S^{17}O_2^{16}O$ and $^{32}S^{18}O^{16}O_2$ for 82.

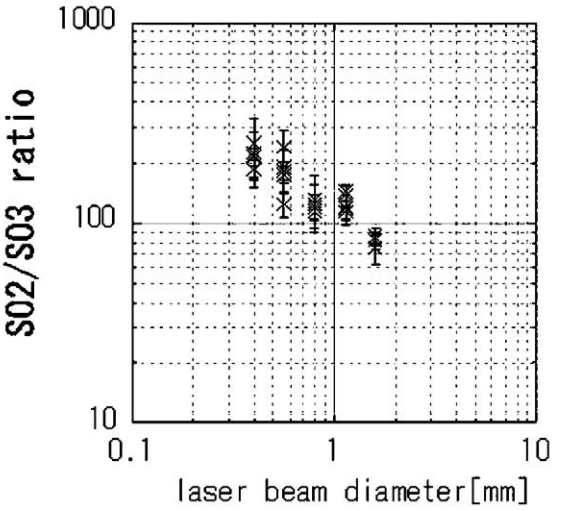

Fig. 7. The SO_2/SO_3 ratios measured in the experiments are shown as a function of laser beam diameters. The error bars in the figure are given by the standard deviation of the time series of the SO_2/SO_3 ratio. The SO_2/SO_3 ratio decreases with the laser beam diameter.

five different beam diameters with a fixed laser intensity per unit surface area in order to determine the effect of the size of vapor clouds on the SO_2/SO_3 ratio. Fig. 7 shows the SO_2/SO_3 ratio measured in the experiments as a function of the laser beam diameter. The gas sample obtained in every laser irradiation experiment was dominated by SO_2, but the significant concentration of SO_3 was also detected. The experimental result reveals that the SO_2/SO_3 ratio decreases as the laser beam diameter increases and that the SO_2/SO_3 ratio was between 80 and 220. These values strongly suggest that the reaction to convert SO_2 to SO_3 experiences a quench near the upper limit of the range of the SO_2–SO_3 transition (Fig. 1).

5. Analysis of the experimental results

5.1. Data fitting

Chi-squared values from least-squares fits to power-law, linear, and exponential functions are 29.5 for a power function, 30.6 for a linear function, and 28.7 for an exponential function, respectively. While the exponential gives a lower chi-squared value, a significance test at the $t(0.01)$ level suggests that a power law is the most likely function assuming a Gaussian distribution of data about each laser beam diameter. The best-fit power law is:

$$SO_2/SO_3 = (116 \pm 3)\left(\frac{D}{1[\mathrm{mm}]}\right)^{(-0.61\pm0.05)} \quad (9)$$

where D is the laser beam diameter. The error of sensitivity calibration of the QMS affects only the coefficient of Eq. 9, i.e., 116 ± 3. The power-law index is not significantly influenced by the sensitivity calibration as long as the output of the QMS is proportional to the concentration of measured gas.

Here the initial mass of a laser-vaporized vapor plume is estimated by $\pi\rho dr^2$ where ρ, d, and r are the density of anhydrite, the thickness of laser-vaporized layer, and the laser beam diameter at the target plane, respectively. Because laser beam irradiation not only vaporizes the anhydrite sample but also cracks and breaks it, it is difficult to determine the depth of vaporization from the remaining anhydrite sample. However, because we maintained the energy flux per unit area and the pulse duration time, the depth of vaporization was expected to be approximately constant. Using this relation, we can convert the diameter scale in Fig. 6 to mass scale. When the experimental data are fitted as a function of vapor cloud mass, we obtain:

$$SO_2/SO_3 = (116 \pm 3)\left(\frac{M}{M_1}\right)^{(-0.31\pm0.02)} \quad (10)$$

where M and M_1 are the mass of the vapor cloud and that of vapor cloud generated by laser irradiation with 1 mm beam diameter, respectively.

5.2. Geometry of the experimental vapor cloud

The rate of expansion and cooling of a vapor cloud is controlled by the effect of geometry. Fig. 8 shows the geometry of an expanding vapor cloud created by laser irradiation. The shape of the initial vapor cloud is a thin disk. The disk-shaped vapor cloud expands isotropically. After it expands sufficiently, the shape of the vapor cloud

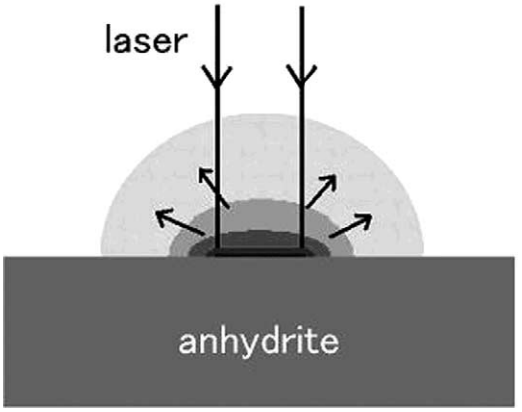

Fig. 8. The geometry of the expanding vapor cloud. The shape of the initial vapor cloud generated by laser irradiation is a thin disk (black zone in the figure). Then the disk-shaped vapor cloud expands. After it expands sufficiently (1 to 10 μs later), the vapor cloud can be approximated as a hemisphere.

becomes hemispherical. If quenching occurred at a very early stage of the expansion of a vapor cloud, the vapor cloud still has a thin disk shape. It is still expanding one dimensionally (vertical to the surface of anhydrite sample). Then, the terminal SO_2/SO_3 ratio and the quenching condition of the experimental vapor clouds do not simulate those of real three-dimensional impact-induced vapor clouds. If the shape of a vapor cloud generated in this study becomes hemispherical at the quenching condition, the terminal SO_2/SO_3 ratio and the quenching condition of the experimental vapor clouds simulate well those of a three-dimensional impact-induced vapor clouds such as the K/T impact vapor cloud.

It is important to assess the geometry of an expanding laser-induced vapor cloud at the time of chemical quenching. However, a new calculation is not necessary because the chemical equilibrium calculations discussed in Section 2 can be used here. The results of chemical equilibrium calculations in Section 2 give the volume of the experimental vapor cloud at the quenching temperature. The volumes of expanding vapor clouds at the quenching temperatures in the experiments are several million times those of the initial vapor clouds. This means that the shapes of the vapor cloud generated in our experiments can be approximated as hemispherical at the quenching temperature.

5.3. Comparison with impact vapor clouds

Vapor clouds generated by laser irradiation are different from those induced by hypervelocity impacts in initial temperature and pressure. Nevertheless, laser-induced vapor clouds may simulate well impact-induced vapor clouds under certain conditions [25]. Vapor clouds generated by laser irradiation have a higher initial temperature than that of hypervelocity impact at the same initial pressure. However, the adiabat that passes the initial condition of an impact-induced vapor cloud always reaches the initial condition of a vapor cloud at higher temperature and pressure. In other words, the initial temperature and pressure of a laser-induced vapor cloud correspond to the temperature and pressure of an adiabatically expanding impact-induced vapor cloud with initial temperature and pressure higher than those of the laser-induced vapor cloud (cf., [25]). If the quenching temperatures are lower than the initial temperatures of laser-induced vapor clouds, the quenching process of chemical reactions in impact vapor clouds can be reproduced in laser-induced vapor clouds. Spectroscopic observation of a laser-induced vapor cloud using Ca emission lines and the method by Sugita et al. [27] reveal the initial temperature is several thousand Kelvin, which is much higher than the expected quenching temperatures. However, because of uncertainty in the equation of state, we cannot determine precisely the initial condition of impact-induced vapor that shares the same adiabat with the laser-induced vapor generated in this study. Nevertheless, the low laser intensity used in this study, which is about 1/33 of that by Kadono et al. [25], generates a vapor plume that simulates an impact-induced vapor cloud with a much lower impact velocity than that (i.e., $\sim$120 km/s) by Kadono et al. [25], assuming comparable impact angles, projectile densities and target densities. Such a moderate impact velocity is more relevant to the K/T impact event. In the following, we discuss the validity of these values and their implications for the K/T boundary event.

6. Implications for the K/T impact event

Fig. 9 compares the SO_2/SO_3 ratio in the model estimation using kinetic theory and the results of the laser irradiation experiment as functions of vapor cloud mass. The SO_2/SO_3 ratio in the experiment is about 1000 times smaller than that in the kinetic model estimation. This occurs presumably because the reaction SO_2+O+M to SO_3+M is not the only reaction path through which SO_2 converts to SO_3. In actual vapor clouds, there may be some other reaction paths that our kinetic model does not take into account.

Fig. 9 also shows that the rate of decrease in the SO_2/SO_3 ratio obtained in the laser experiment as a function of vapor mass is higher than that predicted by the kinetic calculations. The experimental SO_2/SO_3 ratio is approximately proportional to $M^{-0.31}$ where M is the mass of vapor clouds. The kinetic model estimation is approximately proportional to $M^{-0.11}$ in the vapor cloud mass range of our experiment. From these trends, we can estimate the SO_2/SO_3 ratio in a K/T-size impact vapor cloud. The kinetic model calculations predict that the SO_2/SO_3 ratio will be approximately unity (Fig. 2), and the power-low relation obtained in the laser experiments (i.e., Eq. 10) predicts that it will be 10^{-6}.

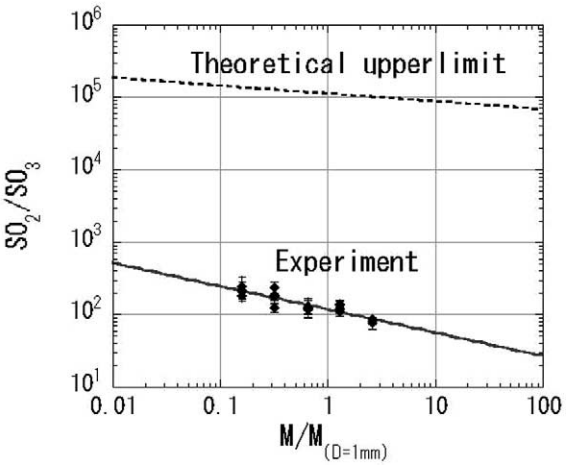

Fig. 9. Comparison between the SO_2/SO_3 ratio measured in the laser experiments and that calculated by the kinetic model as a function of the mass M of a vapor cloud normalized by the mass $M_{D=1\,mm}$ of a vapor cloud generated by laser irradiation with 1 mm beam diameter. The mass of the K/T impact vapor cloud is estimated as 10^{25}–10^{26} times that of the laser irradiation experiment.

If the SO_2/SO_3 ratio in the K/T impact vapor cloud was larger than 1, the mass of SO_2 injected into the stratosphere is more than a half of the total sulfur oxides released by the impact. Then the subsequent processes will not be very different from the previous assessment by Pope et al. [10,11]. The SO_2 mass would be enough to make the blockage of sunlight by sulfuric acid aerosol last for several years. However, the upper limit determined by the kinetic model in this study suggests that the SO_2/SO_3 ratio in the K/T impact vapor cloud can be smaller than 1.

If the SO_2/SO_3 ratio in the K/T impact vapor cloud was smaller than 10^{-2}, the mass of SO_2 injected into the stratosphere by the K/T impact is smaller than that injected into stratosphere by the Toba volcanic eruption about 71 000 years ago, i.e., several gigatons (e.g., [28]). Toba volcanic eruption did not cause a mass extinction. Therefore, if the SO_2/SO_3 ratio in the K/T impact vapor cloud was 10^{-2} times smaller than the kinetic model estimation, the duration of the blockage of sunlight by the sulfuric acid aerosol at the K/T impact event may not have been enough to cause a mass extinction.

If the SO_2/SO_3 ratio in K/T impact vapor cloud was smaller than 1 and larger than 10^{-2}, it is uncertain whether the duration time of the blockage of sunlight by the sulfuric acid aerosol lasts significantly longer than that by the silicate dust. Nevertheless, the dominance of SO_3 may result in the very different scenario from the standard sulfuric acid scenario.

If the experimental trend applies to a K/T-size impact vapor plume, the SO_2/SO_3 ratio will be about 10^{-6} for a K/T-size impact. When the error of the power-law fitting is taken into account, then the error of the SO_2/SO_3 ratio after extrapolation to the K/T-size mass is smaller than a factor of 10. The trend of the SO_2/SO_3 ratio suggests the possibility that SO_3 was dominant in the degassed sulfur by the K/T impact.

However, we need to discuss whether the power law can apply to the K/T-size impact vapor plume or not. The above-mentioned error does not include the possibility that the power law itself does

not hold for the range of 10^{25} of mass. Answering this question requires the knowledge of the kinetics of sulfur oxides over a wide range of temperatures and pressures. Since kinetic data for sulfur oxides are not available particularly at high temperatures and pressures, a theoretical prediction of the SO_2/SO_3 ratio to higher accuracy than in this study is difficult now. Nevertheless, further quantitative discussion is possible. The SO_2/SO_3 ratio obtained in the experiment is much smaller than that in the model calculations. The experimental results also show that the SO_2/SO_3 depends on the vapor mass more strongly than the kinetic model predicts (Fig. 9). This suggests that the SO_2/SO_3 ratio in the K/T impact vapor cloud may have been significantly smaller than our kinetic model estimation, i.e., 1, and that sulfuric acid aerosol may not be able to block the sunlight for a long time. Then the aerosol induced by K/T impact may not contribute to the mass extinction.

The equilibrium SO_2/SO_3 ratio decreases as most minerals (e.g., carbonates or silicates) are added. They (e.g., MgO, Al_2O_3, SiO_2, and CaO) only add O to the system and do not remove O from the system. Chemical equilibrium calculations show that H_2O does not significantly change the SO_2/SO_3 ratio at temperatures (600–2000 K) where conversion from SO_2 to SO_3 is expected to occur, although H_2O dramatically changes the equilibrium chemical compositions at very low temperatures, i.e., lower than 400 K. The results are not expected to change significantly, although the change of reaction rates is uncertain. Experiments by Ivanov et al. [9] suggest that the presence of water may lead to production of sulfuric acid directly from an impact vapor cloud. This also reduces the SO_2 amount in the stratosphere.

Another possible difference between laboratory experiments in this study and a real impact is the presence of the atmosphere. Expansion of a large impact vapor cloud within an atmosphere may lead to large-scale instabilities and turbulence within and outside the vapor cloud (e.g., [29]). It is because the atmosphere will have a large velocity shear with the outward expanding impact vapor. In a radially expanding vapor within vacuum, however, such a velocity difference does not occur. Because the K/T impact vapor cloud was far larger than the scale height of the Earth's atmosphere, the development of intense instabilities and turbulence should be limited within a small portion of the vapor cloud. Thus it will not change the conclusion of this study significantly.

It is still difficult to estimate how long environmental perturbation needs to last to cause a mass extinction. A simple numerical model by Milne and McKay [30] shows that extinction of typical marine planktons requires more than 3 months without sunlight. This timescale can be used as a possible reference on the maximum duration of the effect.

It is noted that one of the 'advantages' of the sulfuric acid aerosol hypothesis is the duration of the resulting perturbation. If the degassed sulfur during the K/T event was dominated by SO_3, however, they should have condensed and formed particles quickly. If most of the sulfuric acid aerosol was formed immediately after the impact, the contribution of sulfuric acid aerosol to the impact winter should have been limited. There are two reasons for this. First, because the visible mass absorption rate of soot and silicate dust is significantly larger than that of pure sulfuric acid aerosol (e.g., [14]), soot and silicate dust are stronger perturbers than sulfuric acid aerosol. For example, Pope et al. [10] shows that blockage of the sunlight by pure sulfuric acid aerosol does not last longer than 1 month and that significant amount of dust/soot contamination is necessary for a long impact winter. Second, because the large quantity of silicate dust ejecta accelerates the growth of sulfuric acid aerosol particles, the residence time of sulfuric acid should be as short as that of silicate dust and soot. The total amount of silicate dust ejecta in the stratosphere immediately after the K/T impact, which is approximately equal to the total mass of global 'fireball layer' in the K/T boundary layer, was very large ($\sim$5 Tt, [7]) and much larger than that ($\sim$100 Gt, [11]) of estimated sulfur oxides released by the K/T impact. Pope [31] estimates that the amount of submicron-size ejecta, which stays in stratosphere for a long period of time, is very small ($<$100 Mt). However, Pope [31] also suggests that the total

amount of silicate dust ejecta (~3.8 Tt) was not necessarily much smaller than the previous estimation (e.g., [7]). These short-lived ejecta may become coagulation nuclei for sulfuric acid aerosol. This will accelerate the coagulation and fall of sulfuric acid aerosol greatly. Consequently, the length of impact winter due to SO_3 would be very small.

Pope et al. [10] shows that the sulfuric acid aerosols grow into large particles rapidly due to the coagulation process and that the duration of the blockage of the sunlight is not longer than 1 month for the case of pure sulfuric acid aerosol. Micron-size silicate dust ejecta accelerates the coagulation process and shortens the duration of the blockage of the sunlight further. However, recent calculations by Pierazzo et al. [14] suggest that the duration of blockage of the sunlight by sulfuric acid aerosol is much longer (i.e., comparable to that for SO_2 cases). Nevertheless, it is not clear why the expected fall time of sulfuric acid aerosol is so different between the model by Pope et al. [10] and that by Pierazzo et al. [14]. Because this difference changes the consequences of sulfuric acid aerosol significantly, it needs to be investigated in the future.

On the other hand, the rapid removal of sulfur oxides from atmosphere may result in another traumatic process; global intense sulfuric acid rain [8,32–34]. The global strong sulfuric acid rain may also have damaged the ecosystem globally and may have contributed significantly to the K/T mass extinction.

Since the results obtained in this study involve extrapolation, the above conclusion should be considered to be still preliminary. Further experiments with larger laser diameters, different laser intensities, and targets with mixtures of $CaSO_4$ and other minerals need to be done before a decisive conclusion can be made. However, the fact that both the model calculation results and the laser irradiation experiment results lead to the same answer (i.e., SO_3 dominance in the K/T impact vapor) is very significant. Such chemical reaction processes within an impact-induced vapor cloud has not been studied extensively before, in particular experimentally. The results of this study underscore the importance of such processes and the need for experimental data on rate coefficients of chemical reactions among gaseous compounds at high temperatures and high pressures.

7. Conclusions

We carried out chemical equilibrium calculations, kinetic model calculations, and laser irradiation experiments in order to estimate the SO_2/SO_3 ratio in the K/T impact vapor cloud. Chemical equilibrium calculations indicate that SO_3 is more stable than $SO_2+1/2{\cdot}O_2$ at low temperatures and low pressures. The kinetic model calculations provide an upper estimate for the SO_2/SO_3 ratio in an expanding impact vapor cloud. The SO_2/SO_3 ratio estimated by the kinetic model for a K/T-size vapor cloud is slightly smaller than unity. Moreover, the SO_2/SO_3 ratio measured in laser irradiation experiments is about 1000 times smaller than that predicted by the kinetic model calculations. The experimental results also show that the terminal SO_2/SO_3 ratio is smaller for a larger mass of impact vapor cloud and that the rate of decrease in the SO_2/SO_3 as a function of mass is greater than that predicted by the kinetic model. These results suggest that the SO_2/SO_3 ratio in K/T impact vapor cloud may have been much smaller than 1 and the sulfuric acid aerosol may not have blocked the sunlight for a long time.

Acknowledgements

The authors thank M. Nakamura for discussion and encouragement and E. Pierazzo and an anonymous reviewer for their careful reviews. This research was partly supported by the Grant in Aide from Japan Society for the Promotion of Science.*[BOYLE]*

Appendix

The fact that SO_3 is more stable than SO_2 at lower temperatures and pressures along an adiabatic decompression line can also be shown by a

simple analytical approach. The Clausius–Clapeyron relation is:

$$\frac{\delta p}{\delta T} = \frac{\Delta_e h}{T \Delta_e v} \tag{A1}$$

where $\Delta_e h$ and $\Delta_e v$ are the changes in enthalpy and molar volume upon chemical reaction [19]. The equilibrium calculation results in Section 2 indicate that only SO_3, SO_2, and O_2 are abundant and the other species such as O, SO, and S are negligible at moderate temperatures and pressures, where freeze-out of chemical reactions may occur. Thus we assume that only SO_3, SO_2, and O_2 are present in the system. If we assume an ideal gas, the increase $\Delta_e v$ in molar volume associated with the reaction from SO_3 to SO_2+1/2·O_2 is:

$$\Delta_e v = \frac{1}{2}\frac{RT}{p} \tag{A2}$$

Because the reaction heat of the reaction from SO_3 to SO_2+1/2·O_2 is approximately constant (102 ± 4 kJ/mol) over a wide range of conditions [20], the integral of Eq. A1 is:

$$\ln p = \frac{-2\Delta_e h}{RT} + C \tag{A3}$$

where C is a constant. In other words, the natural logarithm of the pressure that has a constant SO_2/SO_3 ratio is a linear function of $1/T$.

An adiabatic decompression curve of an ideal gas is written as:

$$\frac{p}{p_0} = \left(\frac{T}{T_0}\right)^{\frac{\gamma}{\gamma-1}} \tag{A4}$$

where γ is the ratio of specific heats, and the subscript '0' denotes the initial condition. When this relation is shown in a $\ln p$–$1/T$ space, it becomes:

$$\ln p = A - \frac{\gamma}{\gamma-1}\ln\left(\frac{1}{T}\right) \tag{A5}$$

Thus logarithmic pressure decreases very slowly (i.e., logarithmically) as the inverse temperature $1/T$ increases. Consequently, the p–T condition given by an adiabatic decompression curve (i.e., Eq. A5) always intersects a contour line (Eq. A3) of a very low SO_2/SO_3 value at a low temperature regardless of the initial condition (cf., Fig. 1). This indicates that SO_3 becomes more stable than SO_2 when an impact vapor cloud is adiabatically decompressed.

References

[1] L.W. Alvarez, W. Alvarez, F. Asaro, H.V. Michel, Extraterrestrial cause for the Cretaceous-Tertiary extinction, Science 208 (1990) 1095–1108.

[2] B.F. Bohor, E.E. Foord, P.J. Modreski, D.M. Tripehorn, Mineralogical evidence for an impact event at the Cretaceous-Tertiary boundary, Science 224 (1984) 867–869.

[3] A.R. Hildebrand, G.T. Penfield, D.A. Kring, M. Pilkington, A.Z. Camargo, S.B. Jacobnsen, W.V. Boynton, Chicxulub crater A possible Cretaceous/Tertiary boundary impact crater on the Yukatan Peninsula, Mexico, Geology 19 (1991) 867–871.

[4] C.C. Swisher, J.M. Grajales-Nishimura, A. Montanari, S.V. Margolis, P. Claeys, W. Alvarez, P. Renne, E. Cedillo-Pardo, F.J.-M.R. Maurrasse, G.H. Curtis, Coeval Ar-40/Ar-39 ages of 65.0 million years ago from Chicxulub crater melt rock and Cretaceous-Tertiary boundary tektites, Science 257 (1992) 954–958.

[5] C. Covey, S.J. Ghan, J.J. Walton, P.R. Weissman, Global environmental effects of impact-generated aerosols; results from a general circulation model, Geol. Soc. Am. Spec. Pap. 247 (1990) 263–270.

[6] C. Covey, S.L. Thompson, P.R. Weissman, M.C. MacCracken, Global climatic effects of atmospheric dust from an asteroid or comet impact on Earth, Glob. Planet. Change 9 (1994) 263–273.

[7] O.B. Toon, J.B. Pollack, T.P. Ackerman, R.P. Turco, C.P. Mckay, M.S. Liu, Evolution of an impact-generated dust cloud and its effects on the atmosphere, in: L.T. Silver, P.H. Schultz (Eds.), Geological Implications of Impacts of Large Asteroids and Comets on the Earth, Geol. Soc. Am. Spec. Pap. 190 (1982)187–200.

[8] H. Sigurdsson, S. D'Hondt, S. Carey, The impact of the Cretaceous-Tertiary bolide on evaporite terrane and generation of major sulfuric acid aerosol, Earth Planet. Sci. Lett. 109 (1992) 543–559.

[9] B.A. Ivanov, D.D. Badukov, O.I. Yakovlev, M.V. Gerasimov, Yu.P. Dikov, K.O. Pope, Degassing of sedimentary rocks due to Chicxulub impact: Hydrocode and physical simulations, Geol. Soc. Am. Spec. Pap. 307 (1996) 125–140.

[10] K.O. Pope, K.H. Baines, A.C. Ocampo, B.A. Ivanov, Impact winter and the Cretaceous-Tertiary extinctions: Results of a Chicxulub asteroid impact model, Earth Planet. Sci. Lett. 128 (1994) 719–725.

[11] K.O. Pope, K.H. Baines, A.C. Ocampo, B.A. Ivanov, Energy, volatile production, and climatic effects of the Chicxulub Cretaceous-Tertiary impact, J. Geophys. Res. 102 (1997) 21645–21664.

[12] E. Pierazzo, Climate forcing from the stratospheric injection of impact-produced sulfur, LPSC32, abstract 1196 (2001).
[13] E. Pierazzo, A.N. Hahmann, Chicxulub and climate: investigating the climate sensitivity of stratospheric injections of impact-generated S-bearing gases, LPSC33, abstract 1269 (2002).
[14] E. Pierazzo, A.N. Hahmann, L.C. Sloan, Chicxulub and climate radiative perturbations of impact-produced S-bearing gases, Astrobiology 3 (2003) 99–118.
[15] D.A. Kring, D.D. Durda, Trajectories and distribution of material ejected from the Chicxulub impact crater: implications for post-impact wildfires, J. Geophys. Res. 107 (2002) E8.
[16] R.P. Turco, P. Hamill, O.B. Toon, R.C. Whitten, C.S. Kiang, A One-Dimensional Model Describing Aerosol Formation and Evolution in the Stratosphere: I. Physical Processes and Mathematical Analogs, J. Atmos. Sci. 36 (1979) 699.
[17] J.A. Tyburczy, T.J. Ahrens, Impact-induced devolatilization of $CaSO_4$ anhydrite and implications for K-T extinctions: preliminary results, LPSC 24 (1993) 1449–1450.
[18] M.V. Gerasimov, Yu.P. Dikov, O.I. Yakovlev, F. Wlotzka, High-temperature vaporization of gypsum and anhydrites: experimental results, LPSC 25 (1994) 413–414.
[19] I. Prigogine, R. Defay, Thermodynamique Chemique, Desoer, Liège, 1944/1950.
[20] M.W. Chase, C.A. Davis, J.R. Downey, D.R. Frurip, R.A. McDonald, A.N. Syverud, JANAF Thermochemical Tables, 3rd edn., J. Phys. Chem. Ref. Data 14, Suppl. 1 (1985) 1–1856.
[21] W. Yang, T.J. Ahrens, Shock vaporization of anhydrite and global effects of the K/T bolide, Earth Planet. Sci. Lett. 156 (1998) 125–140.
[22] J. Troe, Atom and radical recombination reactions, Annu. Rev. Phys. Chem. 29 (1978) 223.
[23] R. Atkinson, D.L. Baulch, R.A. Cox, R.F. Hampson Jr., J.A. Kerr, M.J. Rossi, J. Troe, Evaluated kinetic data and photochemical data for atmospheric chemistry, J. Phys. Chem. Ref. Data 26, Suppl. 6 (1997) 6.
[24] Chemical Society of Japan, Sulfur Oxides, Maruzen, Tokyo, 1975 (in Japanese).
[25] T. Kadono, S. Sugita, N.K. Mitani, M. Fuyuki, S. Ohno, Y. Sekine, T. Matsui, Vapor clouds generated by laser ablation and hypervelocity impact, Geophys. Res. Lett. 29 (2002) 1979.
[26] National Astronomical Observatory, Rika Nenpyo (Chronological Scientic Tables), Maruzen, Tokyo, 1999 (in Japanese).
[27] S. Sugita, P.H. Schultz, Spectroscopic measurements of vapor clouds due to oblique impacts, J. Geophys. Res. 103 (1998) 19,427–19,441.
[28] M.R. Rampino, S. Self, Volcanic winter and accelerated glaciation following the Toba super-eruption, Nature 359 (1992) 50–52.
[29] S. Sugita, P.H. Schultz, Initiation of run-out flows on Venus by oblique impacts, Icarus 155 (2002) 265–284.
[30] D.H. Milne, C.P. McKay, Response of marine plankton communities to a global atmospheric darkening, in: L.T. Silver, P.H. Schultz (Eds.), Geological Implications of Impacts of Large Asteroids and Comets on the Earth, Geol. Soc. Am. Spec. Pap. 190 (1982) 297–303.
[31] K.O. Pope, Impact dust not the cause of the Cretaceous-Tertiary mass extinction, Geology 30 (2002) 99–102.
[32] S. D'Hondt, M.E.Q. Pilson, H. Sigurdsoon, A.K. Hanson, S. Carey, Surface-water acidification and extinction at the Cretaceous-Tertiary boundary, Geology 22 (1994) 983–986.
[33] G.J. Retallack, Acid trauma at the Cretaceous-Tertiary boundary in Eastern Montana, GSA Today 6 (1996) 1–8.
[34] R. Brett, The Cretaceous-Tertiary extinction: A lethal mechanism involving anhydrite target rocks, Geochim. Cosmochim. Acta 56 (1992) 3603–3606.